Available online at www.sciencedirect.com
ScienceDirect
Microporous and Mesoporous Materials 109 (2008) 392–397
MICROPOROUS AND MESOPOROUS MATERIALS
www.elsevier.com/locate/micromeso

Selfassembly of zeolite L crystals on biological self-cleaning surfaces

Olivia Bossart, Gion Calzaferri *

Department of Chemistry and Biochemistry, University of Bern, CH-3012 Bern, Switzerland

Received 10 February 2007; received in revised form 14 May 2007; accepted 15 May 2007
Available online 2 June 2007

Abstract

An interesting phenomenon was observed when the petals of different flowers were immersed into a suspension containing dye-loaded zeolite L crystals. The zeolites align into patterns which are distinct for each flower species. On the petal of a horned pansy, for example, they align into hexagons. Polarised fluorescence microscope images show that the zeolites, to a remarkable extent, are aligned along the hexagonal pattern. We have investigated this in detail and we found that the alignment observed on the flower petals is not due to topological forces. In places which exhibit self-cleaning properties, zeolites are not adsorbed. These observations are new and intriguing. Visualisation of surface patterns by means of optical microscopy methods, which are less destructive than other tools such as electron microscopy, are attractive and may also be applied to living organisms. The phenomenon may also contribute to the application of drugs at specific places, and we can learn from these observations how to pattern a surface in order to realise self-organisation of micro or nano objects.

Keywords: Selfassembly; Zeolites; Fluorescence; Biological microstructure; Surface chemistry; Self-cleaning

1. Introduction

Selfassembly of small objects has been of considerable interest. Organisation of quantum-sized particles, nanotubes, and microporous materials have been studied on different surfaces and used for purposes in science, technology, diagnostics and medicine [1–4]. Size, shape and surface composition of the objects but also the properties of the surface on which they should be organized play a decisive role and in some cases determine not only the quality of the selfassembly but also its macroscopic properties. This has been nicely demonstrated for zeolite L, a crystalline aluminosilicate [5]. Its crystals can been grown in different size and shape which can be described in a simplified manner as having cylindrical morphology; see Fig. 1 [6]. Base and coat of zeolite L have distinctively different chemical properties, and dyes inside the channels are well oriented, facts that have been used for developing new materials [7].

As an example, by subsequent insertion of two different types of dye molecules in a zeolite L monolayer, the first unidirectional antenna system has been realised on a macroscopic scale [8]. Other examples are the hexagonal network organisation of dye-loaded zeolite L crystals by surface tension driven auto-assembly [9], the fluorescent electrospun nanofibres embedding dye-loaded zeolite crystals [10], or arrangements that resemble smectic phases which can be prepared in different ways [11]. We illustrate the consequences of such an arrangement in Fig. 2 where we show the results of an experiment conducted with dye-zeolite L crystals of 6000 nm length. The concept was to align the crystals in a liquid by circulating the zeolite suspension in a tube. The flow rate of a liquid in a tube is different at every point of the cross section. The Poiseuille velocity resembles a parabola due to friction at the tube walls. Due to the different force effects on the elongated crystals they align parallel to the tube walls. Zeolites with an aspect ratio length to diameter of 2.5 were used for the experiment. Half of the amount was loaded with Ox^+

* Corresponding author.
E-mail address: gion.calzaferri@iac.unibe.ch (G. Calzaferri).

1387-1811/$ - see front matter © 2007 Elsevier Inc. All rights reserved.
doi:10.1016/j.micromeso.2007.05.033

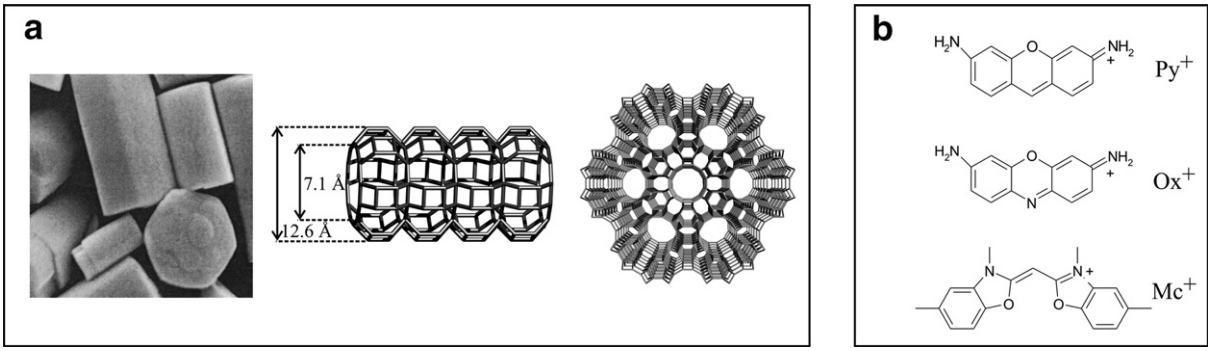

Fig. 1. Zeolite L and some dyes that have been inserted into its channels. (a) Left: SEM image of zeolite L crystals. Middle: Framework side view of a main channel. Right: Framework viewed along the *c*-axis of a crystal with seven main channels (b). Top: pyronine (Py^+). Middle: oxonine (Ox^+). Bottom: methincyanine (Mc^+).

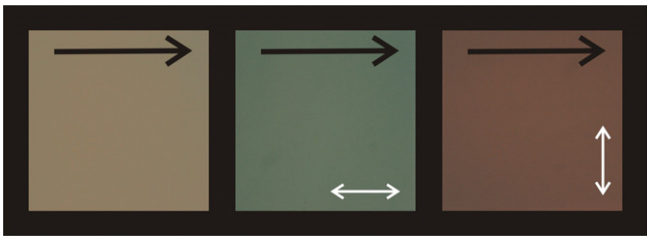

Fig. 2. Fluorescence microscopy images of a suspension containing a 1:1 mixture of Ox^+-zeolite L and Mc^+-zeolite L flowing through a tube. The flow direction is indicated by the black arrows. Left: unpolarised. Middle, right: polarised. The white double arrows indicate the orientation of the transmitted light.

and the other half with Mc^+. The blue fluorescent Mc^+ is aligned parallel to the zeolite channels, while the red fluorescent Ox^+ is smaller and aligned almost perpendicular with respect to the channels [12]. The same amount of each sample was suspended in water and the suspension was pumped through a flexible tube. Between two flexible plastic tubes a quartz glass part was inserted thus enabling microscopic analyses of the suspension flowing through the system. The zeolite suspension was excited from 400 nm to 440 nm and the emission detected through a 475 nm cut-off filter. The intense colour change of the unpolarised and polarised microscope images in Fig. 2 illustrates beautifully the considerable anisotropy of the samples. The images show a section of the quartz plates under the microscope. As the zeolite suspension has a diameter of 1 mm and the crystals are in motion, single particles are not resolved. Similar observations can be made by embedding the same crystals into a PVC polymer film which is then stretched by a factor of 3–5 [13]. The latter experiments resemble to some extent the classical experiments with elongated molecules dissolved in a polymer [14].

Here we describe an interesting phenomenon that was observed when the petals of different flowers were immersed into a suspension containing the same kind of Ox^+-zeolite L crystals as described above: the zeolites align into patterns which are distinct for each flower species.

2. Experimental

Zeolite L crystals were synthesised and characterised as described in Ref. [6]. The potassium exchanged form was used. The experiments were carried out with zeolites of approximately 6000 nm in length and a diameter of 2000 nm. Ox^+ was synthesised and purified according to Ref. [15]. Mc^+ was obtained from CIBA-GEIGY AG. Dye loading of the crystals and quantitative determination of the dye loading was carried out as described in Refs. [7,12]. Zeolite L aligned in a current: approximately 50 mg of dye-loaded zeolites were suspended in 20 mL of doubly distilled water. The suspension was pumped through a tube of 1 mm inner diameter with a peristaltic pump and a pup speed of about 2 mL/min. Two separate batches were loaded, one with Ox^+ and the other with Mc^+. The same amount of each sample was suspended in doubly distilled water and stirred during the experiment. The zeolite suspension was pumped through a flexible tube of 1 mm inner diameter with a peristaltic pump. Between two flexible plastic tubes a quartz glass tube was inserted. The quartz glass was placed under the microscope. Unlike the plastic tube, the quartz glass does not absorb light in the UV, thus enabling microscopic analyses of the suspension flowing through the system. Zeolite L on flower petals and butterfly wings: approximately 50 mg of dye-loaded zeolites were suspended in 20 mL of doubly distilled water. Petals of freshly picked flowers were immersed into the zeolite suspension and dried at room temperature. The same procedure was used to align zeolites on a butterfly's wing. Optical fluorescence microscopy images have been carried out on an Olympus BX 60 device equipped with a Kappa CF 20 DCX Air K2 CCD camera. SEM measurements were carried out by means of scanning electron microscopy (Hitachi S-3000N) at an acceleration voltage of 20 kV. A 3 nm gold layer was deposited on top of the sample.

3. Results and discussion

Petals of different flowers were immersed into a suspension containing the same kind of Ox^+-zeolite L crystals. We

have observed that zeolites align into patterns which are distinct for each flower species when petals of different flowers were immersed into a suspension containing zeolite L crystals. On the petal of a horned pansy (*Viola cornuta*), for example, they align into hexagons, as can be seen on the fluorescence microscope image presented in Fig. 3. The polarised fluorescence microscope images in Fig. 3b shows that the zeolites, to a remarkable extent, are aligned along the hexagonal pattern. SEM images of the same petal were taken. It seems that the zeolites are absorbed into the tissue of the flower. A similar picture was found on the petals of a garden pansy (*Viola wittrockiana*). Even when a large amount of zeolites is deposited onto the petal, the crystals are not distributed over the whole surface but lye in distinct areas only [13].

On the petal of a straw flower (*Helichrysum bracteatum*) the zeolites exhibit quite a different pattern. They align into parallel lanes, as can be seen on the SEM image shown in Fig. 4. The straw flower exhibits elongated epidermis cells. The alignment of the Ox^{+}-loaded zeolites on the straw flower petal can also be observed under the fluorescence microscope. Polarised microscopy images show that most zeolites are oriented in the same direction.

The SEM images of the flowers presented so far give the impression that the zeolites align into patterns due to the surface topology of the petals. This is also the case for the horned pansy, as the intact petal of a horned pansy the papillae stand out like mountains. They collapse when they are subjected to the high vacuum condition in the SEM [13]. On the top side of the petals of a rough hawk's beard (*Crepis biennis*) the zeolites align into parallel lanes, too. A SEM image of the top side of the flower petal containing zeolites is shown in Fig. 5. Again, the alignment of the zeolite crystals could be due to purely topological reasons. However, when examining the bottom side of a rough hawk's beard it becomes apparent, that this is not the case. The bottom side of a rough hawk's beard exhibits rather a smooth topology, but still the zeolites are aligned along the epidermis cells as can be seen in Fig. 5.

An explanation for this behaviour could be the self-cleaning properties of plants. Most parts of a plant are covered by the cuticle which is composed of soluble lipids embedded in a polyester matrix [16]. Due to its chemical composition, the cuticle in most cases forms a hydrophobic surface. Water repellence is mainly caused by epicuticular wax crystalloids which cover the cuticular surface in a regular micro-relief of about 1–5 μm in height [17,18]. Water droplets roll-off the hydrophobic surface of a plant, taking mud, tiny insects and other contaminants with them. This self-cleaning of biological surfaces was described by Barthlott as "Lotus Effect", the lotus flower being a symbol of purity [19]. Before the Lotus Effect was described it was the general opinion that the smoother a surface, the less dirt and water adhere to it. The surface of a lotus leave, however, shows a rough structure on the micro- and nanoscale. Hydrophobic surfaces that are rough on a microscale tend to be more hydrophobic than smooth surfaces due to the reduced contact area between the water and the solid. In the lotus plant for example, the actual contact area is only 2–3% of the droplet-covered surface. The nanostructure is essential to the self-cleaning process: on a smooth hydrophobic surface, water droplets slide rather than roll

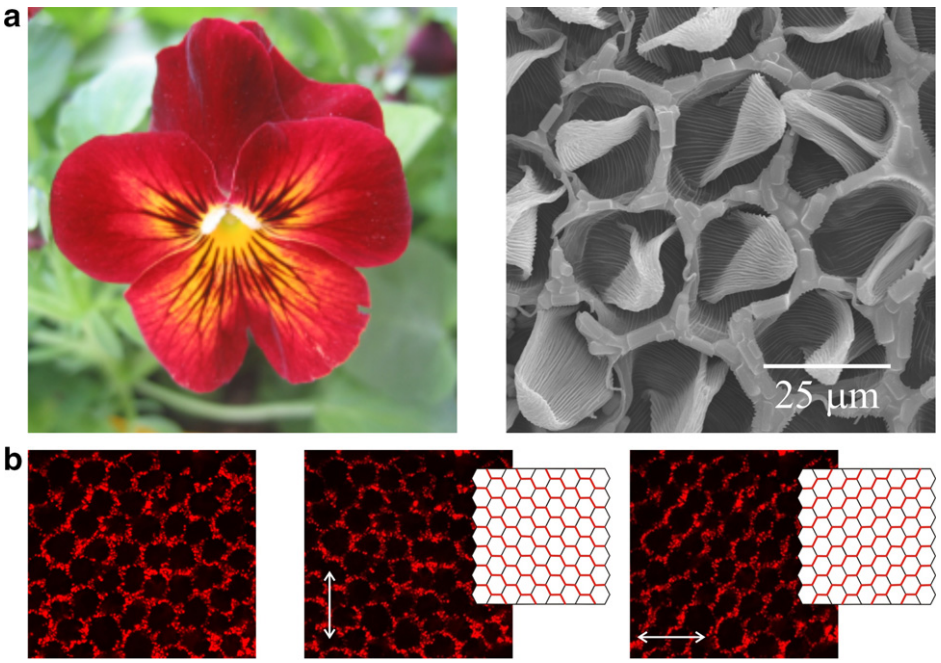

Fig. 3. Horned pansy (*Viola cornuta*). (a) Left: photographic image of a horned pansy. Right: SEM image of a horned pansy petal previously immersed into a zeolite suspension. The zeolites lye on top of the epidermis cell walls. (b) Fluorescence microscope images of Ox^{+}-zeolites aligned on the petal of a horned pansy. Left: unpolarised image. Middle, right: polarised image. The double arrows indicate the orientation of the transmitted light.

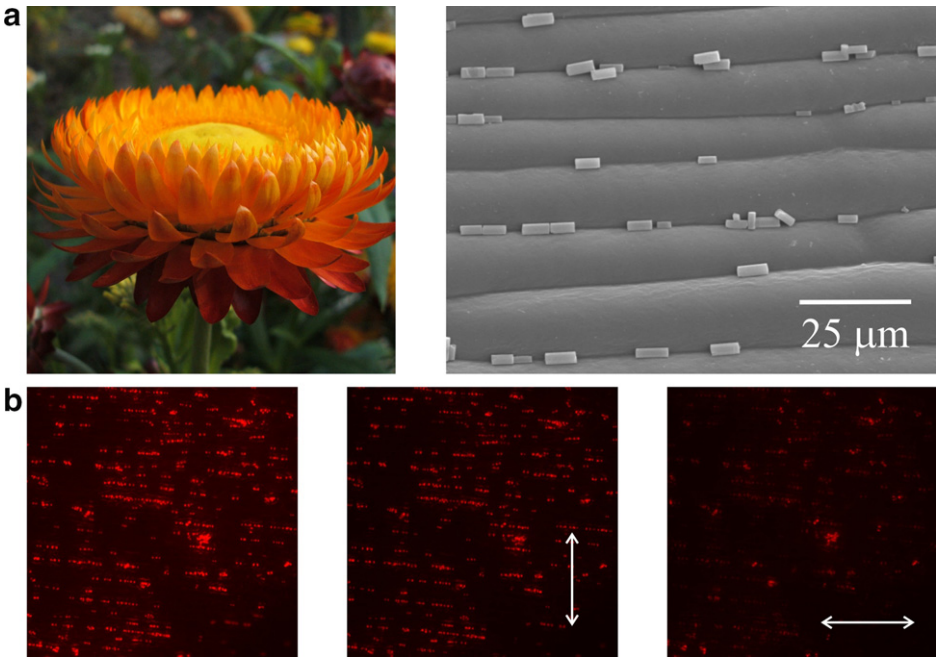

Fig. 4. Straw flower (*Helichrysum bracteatum*). (a) Left: photographic image of a straw flower. Right: SEM image of a straw flower petal previously immersed into a zeolite suspension. The zeolites lye on top of the elongated epidermis cell walls. (b) Fluorescence microscope images of Ox^{+}-zeolites aligned on the petal of a straw flower. Left: unpolarised image. Middle, right: polarised image. The double arrows indicate the orientation of the transmitted light.

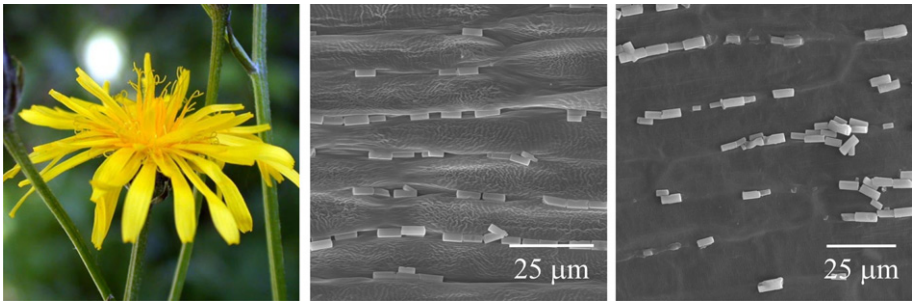

Fig. 5. Rough hawk's beard (*Crepis biennis*). Left: photographic image of a rough hawk's beard. Middle: SEM image of zeolites aligned on the top side of a rough hawk's beard's petal. Right: SEM image of the bottom side of a rough hawk's beard petal containing zeolites.

and do not uptake dirt particles to the same extent as on rough surfaces. Particles have a smaller contact area to a rough surface than to a smooth one. This fact additionally enhances the self-cleaning properties of rough hydrophobic surfaces.

In order to understand the physics behind the Lotus Effect, it is necessary to understand the forces that act upon a drop of liquid on a surface, illustrated in Scheme 1. The contact angle θ is related to these forces and is defined as the angle at which a liquid/vapour interface meets the solid

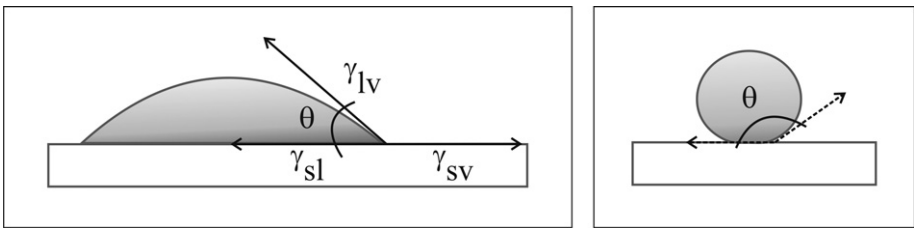

Scheme 1. The contact angle θ is related to the vectors of force between the liquid (l), solid (s) and vapour (v) interfaces. For a non-wetting fluid the contact angle is larger than 90°. It is below 90° for a wetting fluid.

surface. The contact angle is determined by the interactions across the three interfaces solid/liquid, solid/vapour and liquid/vapour. When a water droplet is completely spread on a surface the contact angle is equal to 0°, whereas some highly hydrophobic surfaces exhibit water contact angles as high as 180°. The contact angle of a droplet on a surface is determined by Young's equation [20,21]:

$$\gamma_{sv} - \gamma_{ls} = \gamma_{lv} \cos\theta.$$

For rough surfaces the following relation holds [22]:

$$\cos\theta' = r\cos\theta$$

where r is a roughness factor, defined as the ratio of the actual area of a rough surface to the geometric projected area, and θ' the contact angle of a rough surface. Since r is always larger than unity, the surface roughness improves the wettability of hydrophilic surfaces while the wettability of hydrophobic surfaces decreases.

The self-cleaning property of plants plays a role in the aligning of zeolite crystals on flower petals. It is the reason why no zeolites are found on the epicuticular wax crystalloids. Zeolites are only found along the epidermis cell walls. The primary cell walls and middle lamellas of plants contain pectin, a polar polysaccharide. In the experiments described above, the zeolites are adsorbed to the flower petals from an aqueous suspension. The aqueous zeolite suspension is expected to show a high affinity to the hydrophilic parts of the epidermis cell walls, while it will roll-off the hydrophobic epicuticular wax. This can be shown in a simple experiment which imitates the – strongly simplified – components of the flower petal. A microscope slide was covered with paraffin. With a hypodermic needle small droplets of aqueous pectin suspension were dropped onto the paraffin and dried at room temperature. The microscope slide was then immersed into a zeolite suspension containing dye-zeolites. The paraffin remains dry while the pectin is wetted. Therefore, zeolites are expected to be found only on the pectin droplets. Microscope images taken from such samples confirm this assumption, as illustrated in Fig. 6.

The zeolites themselves are hydrophilic and they exhibit distinctly different chemical properties at the base and the coat of the crystal cylinders. This probably enhances the alignment of the zeolites on the flower petals. In agriculture, the self-cleaning phenomenon of plants is not always welcome. Liquid insecticides or pesticides sprayed onto plant leaves for instance tend to form droplets and roll-off the target. Additionally, it is necessary to add surfactants to the liquid so that the active component can penetrate into the plant. Incorporating active substances into zeolites can be used to release it at specific places at desired rate.

To test the validity of this explanation, we made experiments with wings of butterflies. They are covered with delicate, powdery scales which exhibit an ordered microstructure as can be seen in the SEM images in Fig. 7. The microstructure is responsible for the beautiful colouring of butterflies, which originates from light diffraction and scattering. But it is also due to the microstructure, that the surface of a butterfly's wing possesses water-repellent, self-cleaning or "Lotus Effect" characteristics [23]. The experiment described above was repeated with the wing of a red admiral (*Vanessa atlanta*). Considering the topology which can be seen in the SEM images, zeolites are expected to align into parallel rows. A butterfly wing was immersed into a zeolite suspension. The wing was then examined under the microscope but no zeolites were found on its surface. Only after the wing was immersed into the zeolite suspension several times some zeolites could be observed. The zeolites were only found in places where the scales were no longer intact. Where they still form a consistent area, the zeolites are effectively hindered from adsorbing to the surface. This can be observed under the fluorescence microscope as well as by SEM as can be seen in the bottom left image shown in Fig. 7. After vigorous treatment of the wing in the ultrasonic bath, only few scales are left attached to it. When this damaged wing is immersed into the zeolite suspension, the crystals are found aligned into the microstructure of the scale. As a single scale does not exhibit the self-cleaning property any more, the zeolites can now adsorb to its surface as can be seen in the SEM image presented on the bottom right of Fig. 7.

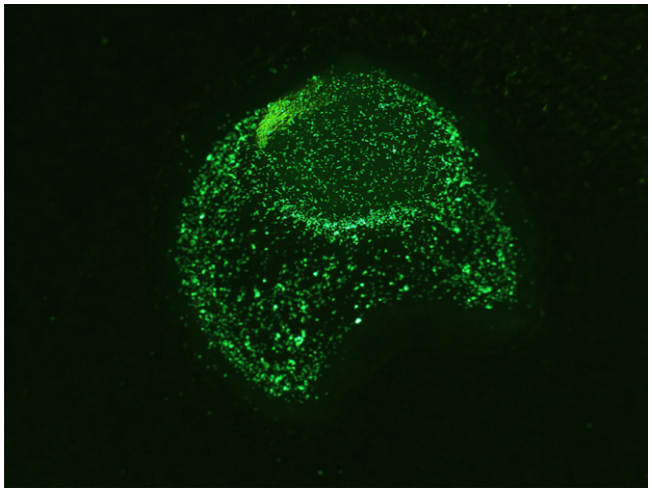

Fig. 6. A pectin droplet on paraffin is covered with zeolites loaded with a green fluorescent dye. No zeolites are found next to the droplet.

These experiments confirm that the alignment which was observed on the flower petals is not determined by topological forces. In places which exhibit self-cleaning properties, zeolites are not adsorbed. These observations are new, intriguing and useful for visualising surface patterns by means of optical microscopy methods, which are less destructive than other tools such as electron microscopy, and may also be applied to living organisms. Another topic of importance is the application of drugs at specific places. Zeolites can be loaded with cations or neutral molecules. Based our observations, such crystals can be adsorbed to certain areas where the inserted molecules are released

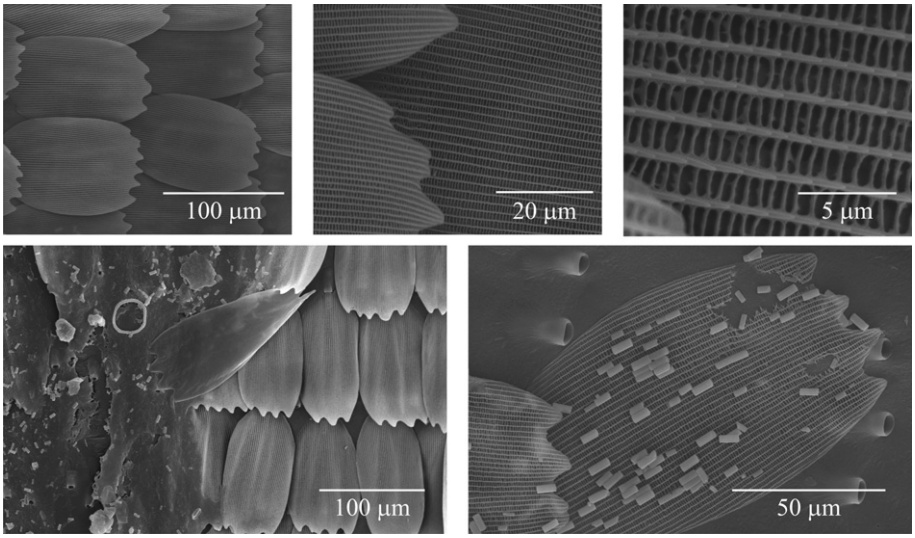

Fig. 7. Experiments made with wings of a red admiral (*Vanessa atlanta*). Top: SEM images of the butterfly's wing which is covered with scales exhibiting an ordered microstructure. Bottom, left: SEM image of a damaged wing containing zeolites. Zeolites and dust particles are only found in areas where the scales are missing. Where the scales form a consistent area, they are still clean. Bottom, right: SEM image of a single scale. The single scale does not exhibit self-cleaning properties. Now the zeolites are aligned along the microstructure of the scale.

under desired conditions. Additionally, we can learn from these observations, how to pattern a surface in order to realise self-organisation of micro or nano objects.

Acknowledgments

This work was supported by the Swiss National Science Foundation NFP 47 (4047-057481). We would like to thank Dr. A. Zabala Ruiz for synthesising the zeolite L and Beatrice Frey for the SEM measurements.

References

[1] (a) M. Bashouti, W. Salalha, M. Brumer, E. Zussman, E. Lifshitz, Chem. Phys. Chem. 7 (2006) 102;
(b) Sheng-Juan Huo, Xiao-Kang Xue, Qiao-Xia Li, Su-Fan Xu, Wen-Bin Cai, J. Phys. Chem. B 110 (2006) 25721;
(c) L. Dai, A. Patil, X. Gong, Z. Guo, L. Liu, Y. Liu, D. Zhu, Chem. Phys. Chem. 4 (2003) 1150.
[2] (a) G.A. Ozin, A.C. Arsenault, Nanochemistry, a chemical approach to nanomaterials, in: RCS, ISBN 0-85404-664-X, 2005;
(b) S.J. Hurst, E.K. Payne, L.D. Qin, C.A. Mirkin, Angew. Chem. Int. Ed. 45 (2006) 2672;
(c) T. Bein, Zeolitic host–guest interactions and building blocks for the selfassembly of complex materials, MRS Bull. 30 (2005) 713;
(d) A. Walcarius, V. Ganesan, O. Larlus, V. Valtchev, Electroanalysis 16 (2004) 1550;
(e) A. Gouzinis, M. Tsapatsis, Chem. Mater. 10 (1998) 2497.
[3] (a) K.B. Yoon, Acc. Chem. Res. 40 (2007) 29;
(b) J.S. Lee, H. Lim, K. Ha, H. Cheong, K.B. Yoon, Angew. Chem. Int. Ed. 45 (2006) 5288.
[4] C. Leiggener, G. Calzaferri, Chem. Phys. Chem. 5 (2004) 1593.
[5] (a) Ch. Baerlocher, W.M. Meier, D.H. Olson, Atlas of Zeolite Framework Types, fifth ed., Elsevier, Amsterdam, 2001;
(b) T. Ohsuna, B. Slater, F. Gao, J. Yu, Y. Sakamoto, G. Zhu, O. Terasaki, D.E.W. Vaughan, S. Qiu, C.R. Catlow, Chem. Eur. J. 10 (2004) 5031;
(c) O. Larlus, V.P. Valtchev, Chem. Mater. 16 (2004) 3381;
(d) C.S. Carr, D.F. Shantz, Chem. Mater. 17 (2005) 6192.
[6] (a) A. Zabala Ruiz, D. Brühwiler, T. Ban, G. Calzaferri, Monatshefte für Chemie 136 (2005) 77;
(b) A. Zabala Ruiz, D. Brühwiler, LQ. Dieu, G. Calzaferri, in: U. Schubert, R.M. Laine, N. Huesing (Eds.), MATSYN, Wiley, in press.
[7] G. Calzaferri, S. Huber, H. Maas, C. Minkowski, Angew. Chem. Int. Ed. 42 (2003) 3732.
[8] (a) A. Zabala Ruiz, H. Li, G. Calzaferri, Angew. Chem. Int. Ed. 45 (2006) 5282;
(b) S. Huber, A. Zabala Ruiz, H. Li, G. Patrinoiu, Ch. Botta, G. Calzaferri, Inorg. Chim. Acta 360 (2007) 869.
[9] S. Yunus, F. Spano, G. Patrinoiu, A. Bolognesi, Ch. Botta, D. Brühwiler, A. Zabala Ruiz, G. Calzaferri, Adv. Funct. Mater. 16 (2006) 2213.
[10] I. Cucchi, F. Spano, U. Giovanella, M. Catellani, A. Varesano, G. Calzaferri, Ch. Botta, Small 3 (2007) 305.
[11] O. Bossart, G. Calzaferri, Chimia 60 (2006) 179.
[12] C. Minkowski, G. Calzaferri, Angew. Chem. Int. Ed. 44 (2005) 5325.
[13] O. Bossart, Zeolite L antenna material for organic light emitting diodes and organic solar cells, Ph.D. thesis, 2006, University of Berne.
[14] J. Michl, E.W. Thulstrup, Acc. Chem. Res. 20 (1987) 192.
[15] H. Maas, A. Khatyr, G. Calzaferri, Micropor. Mesopor. Mater. 65 (2003) 233.
[16] P.J. Holloway, in: K.E. Percy, J.N. Cape, R. Jagels, C.J. Simpson (Eds.), Air Pollution and the Leaf Cuticle, Springer, Berlin, 1994, pp. 1–13.
[17] E.A. Baker, in: D.F. Cutler, K.L. Alvin, C.E. Price (Eds.), The Plant Cuticle, Academic Press, London, 1982, pp. 139–166.
[18] C.E. Jeffree, in: B.E. Juniper, S.R. Southwood (Eds.), Insects and the Plant Surface, Edward Arnold, London, 1986, pp. 23–63.
[19] W. Barthlott, C. Neinhuis, Planta 202 (1997) 1.
[20] T. Young, Philos. Trans. R. Soc. London 95 (1805) 65.
[21] D.H. Bangham, R.I. Razouk, Trans. Faraday Soc. 33 (1937) 1459.
[22] R.N. Wenzel, Ind. Eng. Chem. 28 (1936) 988.
[23] (a) Z.-Z. Gu, H. Uetsuka, K. Takahashi, R. Nakajima, H. Onishi, A. Fujishima, O. Sato, Angew. Chem. Int. Ed. 42 (2003) 894;
(b) L. Jiang, Y. Zhao, J. Zhai, Angew. Chem. Int. Ed. 43 (2004) 4338;
(c) Y. Zheng, X. Gao, L. Jiang, Soft Matter 3 (2007) 178.